Numerical simulation of hygrothermomechanical deformations of bituminous pavements in the city of Ouagadougou subjected to tropical dry showers

Abbreviations

NR2 : national road 2

NR4 : national Road 4

KP : kilometric point

AC : asphalt Concrete

BC : grave bitumen

LITHO : lithostab

LGC : lateritic Clayey Gravels

BRT : ball ring temperature

HGH : heavy weights

I_p : plasticity index

I_{CBR} : California Bearing Ratio index

Nomenclature

ϵ_T : total strains

C_p : heat capacity (J $kg^{-1}K^{-1}$)

h_c : convective exchange coefficient

Comment [BI1]: Abbrevation can be explained at first mention in the text. Listing of abbreviation is only appropriate for a thesis or project

I_c : sky clarity index

P_v : vapor partial pressure(Pa)

R_g : incident solar radiation (W/m^2)

$\overline{T}$: hourly average air temperature (°C)

T_{rain}: the temperature of the rainwater (°C)

T_{air} : température de l'air (°C)

T_s : air temperature (°C)

T_{sky} :sky temperature (°C)

T_z : temperature at depth z (m)

V_{Wind} : wind speed $\left(\frac{m}{s}\right)$

α_{th} : coefficient of thermal expansion

ϵ_m : mechanical strains

ϵ_{th} : thermal strains

φ_{conv} : coefficient of longitudinal friction (W/m^2)

A : temperature range (°C)

D : thermal diffusivity of the layer (m^2s^{-1})

k : thermal conductivity $(Wm^{-1}K^{-1})$

T : temperature (°C)

t : time (s)

x : axis of the pavement according to the length (m)

z : axis of pavement by depth (m)

α : albedo of the pavement surface

ϵ : emissivity of the pavement surface

ρ : density of pavement course $(kg\ m^{-3})$

ρ_{water} : water density $(kg\ m^{-3})$

σ : Stefan-Boltzmann constant $5.669 \times 10^{-8}\ (Wm^2K^{-4})$

φ : phase

E : modulus of rigidity (Pa)

e : thickness of the layer (m)

v : poisson ratio

τ : period of daily fluctuations (s)

ω : daily pulse (s^{-1})

φ_{rain}: energy taken by rainfall

φ_e : energy extracted from rainwater evaporation

$C_{p_{water}}$: thermal capacity of water$(J\ Kg^{-1}K^{-1})$

T_r : the return frequency (year)

i : rain intensity (mm/h)

h_{fg}: latent heat of vaporization $(kJ\ kg^{-1})$

HR_{air} : relative humidity of the ambient air (%)

HR_s : humidity of the saturated air on the surface of the pavement (%)

$\dot{m}_{eau}$: water mass flow (kg/m^3)

Abstract

Rain-related degradation of bituminous pavements is often observed in the city of Ouagadougou. The objective of this article is to estimate, as a first approach, the effect of tropical rains on the thermomechanical behaviour of bituminous pavements formulated with pure grade 35/50 bitumen and grade 10/65 modified bitumen without trafic.

The bituminous pavements studied were subjected to maximum rainfall intensities of 53.06 mm/h, and 99 mm/h with respective frequencies of occurrence of 2 years and 15 years.

The comparison of the temperature profiles at the surface of the studied pavements, allowed to highlight the more or less viscous character of the asphalt subjected to the rains of maximum intensity of 99 mm/h. The maximum deformations simulated during these rains are about 1.2 times greater in the wearing course than in the base course, which does not disrupt the classical order of temperature evolution in the different pavement layers under dry tropical conditions. These deformations obtained also respect the admissibility criteria in terms of pavement design for T2 traffic (151 to 300 HGV/day).

Keywords : pavement, hygrothermomechanical, modeling, dry tropical weather

1. INTRODUCTION

The modeling of hygrothermal transfers in pavements appears in the literature as an extended study of thermal transfers. Heat transfer in pavements depends on meteorological conditions, including precipitation.

To our knowledge, researchers studying heat transfer in pavements do not always take into account precipitation in the weather conditions. Taking precipitation into account would allow all meteorological conditions to be considered for the prediction of pavement temperature. The modelling of hygrothermal transfers makes it possible to propose to pavement design engineer's calculation tools that increase the accuracy of temperature prediction for a more rigorous pavement design [1].

Two approaches are used to evaluate the action of water on pavement temperature. In the first approach, researchers assume that the flow of the water film from precipitation is instantaneous and that there is no accumulation of rain on the pavement surface [1,2].

In a second approach, others try to study the transfer mechanisms during precipitation [3,4,5].

Yavuzturk et al. [1] developed a two-dimensional numerical model based on the finite difference method to predict temperature fluctuations at different depths and lateral locations in bituminous pavements. This model is unique in that it accounts for the energy flux from precipitation in the energy balance at the pavement surface. Hourly temperatures at any arbitrary point on a bituminous pavement are obtained by taking into account weather conditions, pavement geometry and orientation. In 2005, Yavuzturk et al [6] improved the model by additionally evaluating the thermal deformations associated with these thermal fluctuations. Subsequently, [2] refined the [6] model to account for the thermal effects of the pavement surface slope angle with respect to the horizontal, heat transfer from the pavement surface due to precipitation, and to provide estimates of thermal deformations in multilayer pavements due to thermal environmental conditions.

This model showed that precipitation and evaporation have a significant cooling effect on pavement surface temperatures and that thermal stresses on asphalt pavements are strongly impacted by the thermal conductivity of the asphalt layers and their location in the pavement structure. They also demonstrated that the pavement slope angle can have a significant impact on the pavement temperature distribution. Depending on the surface, azimuth, temperatures on a sloped surface will be seasonally higher or lower than temperatures on a horizontal surface.

Heat transfer mechanisms over pavements during precipitation are poorly understood due to difficulties in capturing the many important physical processes and parameters in experiments and models.

Van buren et al, Cohard et al. [3,4] proposed heat transfer models including all surface energy balances to calculate soil surface temperature during precipitation and estimated runoff temperature as a function of precipitation and pavement surface temperature.

Comment [BI2]: Not consistent with the reference style

Comment [BI3]: ditto

Comment [BI4]: same as above

Similarly, Janke et al. [4] suggested a more comprehensive model solving a one-dimensional (1D) runoff model numerically coupled with a 1D heat balance for the subsurface and runoff.

Kertesz and Sansalone [7] used field measurements performed on asphalt pavements in conjunction with a heat balance model that combines the models used in the studies of Van buren et al., Janker et al., Herb et al., Kim et al., Sansalone and Teng, Thompson et al. 2008[3,4,8,9,10] to investigate the transfer of thermal energy in the pavement during rainstorms.

In the previously cited studies, the runoff is in an equilibrium state with the surface (no vertical temperature gradient was assumed in the runoff) and no infiltration was allowed. They do not take into account the dynamics of the flows, more precisely the equations of the flows taking place according to the depth and the speeds of runoff.

Omidvar et al [12] developed a detailed two-dimensional model of heat and water transfer processes in impermeable bituminous pavement. This model that takes into account runoff dynamics along the vertical showed that the temperature difference between the pavement surface and runoff water can be larger or smaller for wide pavements and short duration precipitation (because the thickness of runoff water downstream is greater than upstream). The model also indicated that the driving heat transfer processes for the runoff layer are heat gain from the pavement surface and heat loss from the net cooler precipitation flow and the warm runoff flow. Cooling by latent heat from the pavement was a secondary but not insignificant factor, while net radiation and sensible heat flux were insignificant under realistic, cloudy rainfall conditions.

Comment [BI5]: inconziztent

The disastrous effect of tropical downpours on asphalt pavements in hot and dry tropical areas is well documented.

The objective of this article is to evaluate the thermomechanical deformations associated with rainfall in the city of Ouagadougou on national roads 1 and 2 made of asphalt mixes.

The thermomechanical deformations that will be quantified will be compared to the permissible deformations proposed by the practical guide for the design of tropical pavements in order to estimate the unique effect of rain on the deterioration condition of new asphalt pavements.

2. MATERIALS AND METHODS

2.1 Materials

Within the framework of this work, the national roads 1 and 2 of the city of Ouagadougou, were studied. These are the sections located between kilometric points KP2+675 and KP2+850, with a length of 175 meters for the NR4 ; and kilometric points PK00 and PK00+275, with a length of 275 meters for the NR2. The NR4 is located to the west of the city and can be identified by the following geographical coordinates N 12.34359°, W 001.56948°. The RN2 is located to the north of the city of Ouagadougou with the following geographical coordinates N 12.38836°, W 001.48810°. From a geotechnical point of view, both pavements are flexible and made up of four (4) layers: a wearing course and a base course in bituminous mix, a sub-base course above the subgrade soil.

The different materials of the pavement layers were reconstituted in the laboratory from the formulas used by road builders.

Comment [BI6]: do you mean stone based course (concrete base)

2.1.1 Bitumen

Pure 50/70, 35/50 and modified 10/65 bitumens were used in the design of the surface courses.

The characteristics of these bitumens are listed in Table 1.

Table 1. Bitumen identification.

Comment [BI7]: use table design to remove lines Source?

Layer	Bitumen grade	ρ (kg/m³)	Penetrability (°C)	BRT (°C)
AC and BC NR4	35/50	1025	38.66	54.75
AC-NR2	10/65	1.026	27.16	65.5
BC- NR2	35/50	1.018	37.83	54.25

2.1.2 Asphalt concrete layers

The asphalt mixes used in the wearing course and the base course are composed of a mixture of crushed granite and bitumen. The granites used for the asphalt mixes of the two pavements come from different quarries. The granites for the NR4 are from the Yimdi quarry, located at N 12.30098°, W 001.69862° and those for the NR2, from the Yagma quarry, located at N 12.38555°, W 001.55814°.

The formulas of the asphalt layers, coming from the data of the road builders, are arranged in the tables (table 2 and table 3).

Table 2 : Composition of asphalt mixes for the NR4.

Asphalt Concrete (AC)		
	Components	Dosage (%)
	6/10	43.3
	4/6	16.5
	0/4	34
	Bitumen 50/70	5.2
Grave Bitumen (BC)		
	Components	Dosage (%)
	10/14	33

Table 3 : Composition of asphalt mixes for the NR2.

Asphalt Concrete (AC)		
	Components	Dosage (%)
	6/10	38.69
	4/6	15.86
	0/4	45.45
	Bitumen 10/65	5.4
Grave Bitumen (BC)		

Comment [BI8]: Separate Table 3 from Table 2 and desgn table to remove lines

	Components	Dosage (%)
	10/14	28.7
	4/10	20
	0/4	45
	Bitumen 35/50	4.3

2.1.3 Sub-base course and soil subgrade

The subgrade is obtained by lithostabilization [13].

The Lithostab (LITHO) used in this work is a mixture of 30% crushed granites and lateritic clayey gravels (LGC) from Yimdi at N 12.31131°, W 001.65680° for NR4 and from Banogo at 12° 18' 14" for NR2. The subgrade is exclusively composed of the same gravelly clayey lateritic material.

The geotechnical properties are recorded in table 4.

Table 4. Geotechnical characteristics of the LITHO and LGC.

Comment [BI9]: ditto

Mixes Identification		Size distribution (%)			Plasticity index I_P (%)	Optimum Modified Proctor		I_{CBR} at 95% OPM
		0.08 mm	2 mm	10 mm		w_{OPM} (%)	ρd (g/cm³)	
NR4	LITHO	16	32	70	15	7.3	2.24	68
NR4	LGC	19	36	86	16	7.1	2.15	49
NR2	LITHO	24.5	48.5	87.5	13	9.4	2.12	68
NR2	LGC	18	40	79	14	7.4	2.15	41.5

2.2 Methods

The work carried out in this article was carried out in three steps corresponding to the mathematical formulation of the problem, the determination of the parameters (geotechnical and thermophysical meteorological) necessary for the implementation followed by the numerical simulation using the Comsol Multiphysics 5.2 software (Fig.1.).

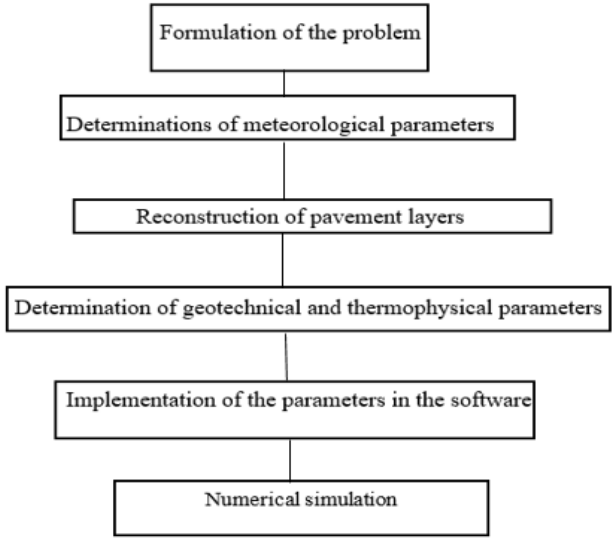

Most of the geotechnical and thermophysical parameters were obtained after a laboratory reconstruction of the pavement layers.

Fig. 1 : Schematic representation of the methodoly.

2.2.1 Statistical analysis of rainfall data

The first data on rainfall provided by the meteorological services of Burkina Faso is the height of water falling per day, the sum of the heights collected in 24 hours (from 6:00 a.m. UTC on the day to 6:00 a.m. the next day). This data does not allow us to determine the number associated with the duration of the rain. For this purpose, the most unfavorable quantifiable rainfall hypothesis is made. It is assumed that the daily amount of water obtained from the meteorological services is associated with a single shower of 3 hours' duration.

According to the work of Bourier [14], when rainfall records are available (duration of the shower, height of water fallen), the average intensity of each rainfall can be known, which is generally acceptable for short duration showers but quite random for long duration rainfall. For a given time interval, the synthetic hyetogram was determined by Talbot's homographic formula because it is adapted for rainfall intensities of less than 24 hours [14]

$$i(t) = \frac{a(T_r)}{t+b(T_r)} \quad (1)$$

$a(T_r)$, $b(T_r)$ are the Montana coefficients by linear regression of $\ln(i(t)$ gainst time t for the return frequency T_r.

The intensity profile was then defined from the Desbordes project rainfall model [15] adapted to African tropical rains according to the work of [16] whose duration is less than or equal to 3 hours (Fig. 2).

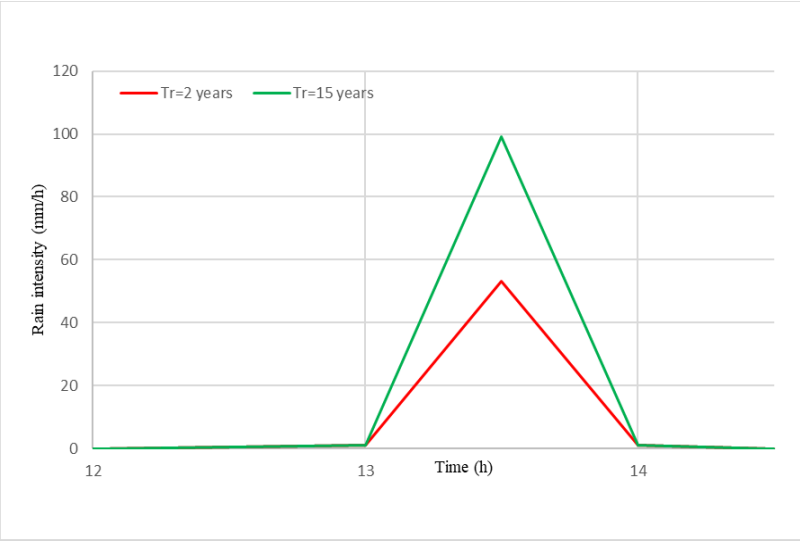

Fig. 2. Intensity profile was then defined from the Desbordes project rainfall model [15]

Comment [BI10]: should be placed under the Figure

Comment [BI11]: Take the section to thr next page

2.2.2 Numerical model

When the pavement is subjected to a rainfall event, additional energy is added to the energy available at the pavement/atmosphere interface **(Fig. 3)**. These are the energy induced by the rainwater falling on the pavement and the energy related to the evaporation of the water present on the pavement surface.

Furthermore, it is assumed that drainage occurs instantaneously in a laminar flow and that infiltration and runoff phenomena are not taken into account in the model.

The heat transfer in the different layers of the pavement is therefore governed by the radiative energies exchanged between the surface and the atmosphere and the energies previously described: the absorbed energy, the energy emitted by the surface towards the sky, the energy induced by the rainfall, the energy produced by the evaporation of a thin film of water available on the surface.

The pavement is often considered in the literature as a semi-infinite, isotropic, linear, low-temperature viscoelastic, water-impermeable homogeneous solid medium [17]. It is not expected to produce energy translated into zero internal heat flux (zero geothermal gradient) [18]. It is subject to local weather conditions. The assumption of perfect contact between layers results in temperature continuity and heat flux conservation at the interfaces between two successive layers in the linear thermoelastic model with a rainwater film.

The proposed linear thermoelastic numerical model can be represented schematically as shown in Fig. 3.

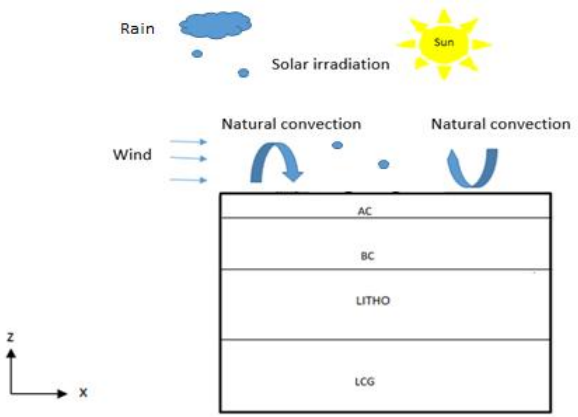

Fig. 3 : linear thermoelastic numerical model with rain.

2.2.2.1 The mathematical formulation of the problem

The physical problem posed in this article a thermal problem leading to a mechanical behaviour.

Comment [BI12]: Check the numbering of subsections

2.2.2.1.1 Formulation of heat transfer phenomena

The equation governing the heat transfer in the different layers of the pavement is given by :

$$\Delta T = \frac{1}{D}\frac{\partial T}{\partial t} \qquad (2)$$

2.2.2.1.1.1 Energy balance in the pavement

The pavement is subject to weather and traffic conditions. Under these conditions, the net energy φ_{net} (W/m^2) available at its surface which is then transferred by conduction to the different layers is given by the following relation [19] :

$$\varphi_{net} = \varphi_a + \varphi_r + \varphi_{cond} \pm \varphi_{conv} + \varphi_{rain} + \varphi_e \quad (3)$$

φ_a : energy absorbed by the pavement from direct solar radiation

φ_r : energy emitted from the pavement to the sky

φ_{cond} : energy transferred to the pavement by conduction

φ_{conv} : energy transferred to the pavement by convection

φ_{rain} : energy taken by rainfall

φ_e : energy extracted from rainwater evaporation

2.2.2.1.1.2 Heat flux absorbed by the pavement

There are two components to solar radiation incident on the pavement surface :

The sun emits short-wave radiation onto the pavement surface. Part of its energy is absorbed by the pavement surface causing a rise in the pavement temperature. This energy is given by :

$\varphi_a = (1-\alpha)R_g$ Where α is the albedo and R_g the global radiation (4)

In our case, the albedo of the road surface is equal to 0.18 [17].

The pavement in turn emits long wave radiation to the sky according to the Stefan-Boltzmann law :

$$\varphi_r = \sigma\epsilon\left(T^4_{sky} T^4_s\right) \quad (5)$$

with σ is the Boltzmann constant, ϵ the emissivity of the pavement surface, T_{sky} , sky temperature , T_s the temperature at the surface of the pavement, ϵ The emissivity of the pavement surface is taken equal to 0,92 [17] ;

The sky temperature is given by [20] :

$$T_{sky} = 94.12 \ln(P_v) - 13\, I_c + 0.314 T_{air} \quad (6)$$

where P_v is the vapor pressure, I_c is the sky clarity index and T_{air} is the air temperature

2.2.2.1.1.3 Heat flux transmitted to the pavement by conduction

The energy flow obtained by conduction φ_{cond} at the pavement surface can be approximately calculated by the following relationship [21] :

$$\varphi_{cond} = -k\frac{T_z - T_s}{z} \quad (7)$$

with k the thermal conductivity of the layer, T_z the temperature at depth z

2.2.2.1.1.4 Heat flow generated by convection phenomena

Natural convection is a transfer of energy between the air and the pavement surface.

The convective energy is given by Newton's law :

$$\varphi_{conv} = h_c(T_s - T_{air}) \quad (8)$$

With h_c the convective exchange coefficient

The wind speed, V_{wind} of the city of Ouagadougou, is generally below 5 m/s at 30 m from the ground [22], therefore the expression of the convective exchange coefficient [17, 18] is the following

$$h_c = 5.8 + 4.1 \times V_{wind} \quad (9)$$

2.2.2.1.1.5 energy taken by rainfall

Rainfall causes energy to be deposited on the pavement surface. This energy is related to the intensity of the rain and the thermal gradient between the surface temperature and the rainwater. It is given by the following relation [2]:

$$\varphi_{rain} = 3{,}6 \times 10^{-6} \times i \times \rho_{water} \times C_{p_{water}} (T_{rain} - T_s) \quad (10)$$

i is the intensity of the rain; ρ_{water} the density of the water; $C_{p_{water}}$ thermal capacity of water; T_{rain} the temperature of the rainwater.

2.2.2.1.1.*6* **energy extracted from rainwater evaporation**

Rainwater droplets that hit the surface of the pavement form a sheet of water that can evaporate or run off. The evaporation of the water causes the pavement to cool. The energy produced by the evaporation mechanism is given by the following relationship [2,6]:

$$\varphi_e = h_{fg} \times \dot{m}_{water} \quad C_{p_{water}} (HR_{air} - HR_s) \quad (11)$$

h_{fg} is the latent heat of vaporization,HR_{air} the relative humidity of the ambient air, HR_s the humidity of the saturated air on the surface of the pavement. The values of $\dot{m}_{eau}$, HR_s were determined using empirical value tables [23].

2.2.2.1.2 Strains

The thermal stresses induced by heat transfer are given the following relationship [24]:

$$\epsilon_T = \alpha_{th} \Delta T \quad (12)$$

with α_{th} the coefficient of thermal expansion and ΔT the temperature variation at the surface of the layer

2.2.2.2 Linear thermoelastic model of pavement subjected to rain

The numerical model is built on the finite element method using the COMSOL Multiphysics 5.2 software. The input data are the geometrical characteristics of the pavement, the thermophysical and geotechnical properties of the materials, the hourly evolution of the meteorological parameters as well as the braking parameters obtained from the mathematical formula of the problem.

The output parameters are the temperature, displacement and deformation fields associated with precise positions in the different layers of the pavement such as the surface of the wearing course, the interface between the wearing course and the base course, the middle of the sub-base and the subgrade soil.

2.2.2.2.1 The initial temperature condition

The initial condition chosen, was obtained by theoretical calculation [25] from the general solution of the heat equation (1) can take the following real form :

$$T(z,t) = \overline{T} + A\sin\left(\omega t - \varphi(z)\right) \text{ [26]} \quad (13)$$

$$A = A_0 e^{-kz} \text{ with } A_0 \text{ is the daily temperature amplitude ;} \quad (14)$$

$$\varphi = kz \text{ is the phase ;} \quad (15)$$

$$k = \sqrt{\frac{\pi}{D\tau}} \quad (16)$$

The results are reported in table 5.

Table 5. Determined initial temperatures of the different layers.

$\overline{T}$ at 06:00 am	A_0	T_{BB}	T_{GB}	T_{LITHO}	T_{GAL}
23.8°C	19.5°	21.1°C	15.7°C	15.6°C	15.6°C

2.2.2.2.2 Meteorological and geometrical parameters of the model

The meteorological data used for the simulations come from the National Directorate of Meteorology of Burkina Faso.

These are hourly values from 6 am to 6 pm of solar radiation, air temperature, dew point temperature, air humidity, wind speed.

The numerical model built is two-dimensional, it takes into account the thickness and length to be simulated when the pavement is dry.

2.2.2.2.3 Thermo-physical and geotechnical parameters of the model

he thermal conductivities of the four layers were measured while the other thermo-physical parameters such as the coefficient of thermal expansion [24] and the specific heat capacity were taken from the literature [27,28].

It should be noted that the stiffness moduli of the bituminous concrete were obtained experimentally according to the protocol described in the work of koudougou et al. [29].

The moduli of the foundation and subgrade layers are obtained by applying the empirical relations [18]. They are assumed to be temperature invariant.

The geotechnical and thermo-physical properties of the surface layers are listed in Table 6.

Table 6. Summary table of thermo-physical and geotechnical pavement data.

	Pavement layer	**e**	**E**	**ν**	**k**	**C_p**	**ρ**	**α_{th}**
		cm	Pa		W /mK	J/kg/°C	kg/m^3	$\frac{\mu m}{m}/°C$
NR4	AC	4	$-1018.1T^3 + 181094T^2 - 10^7$	$0.15 + 0.35/(1 + \exp(3.1849 - 0.04233\,T(°F)))$ a	1.702	900a	2260	2.10^{-5}c
	BC	15	$-1181.1T^3 + 210294T^2 - 410^7$	$0.15 + 0.35/(1 + \exp(3.1849 - 0.04233\,T(°F)))$ a	1.584	900a	2300	2.10^{-5}c
	LITHO	20	34×10^8	0.4_b	0.77	900b	2240	
	LGC	20	14.70×10^8	0.4_b	0.67	600b	2120	
NR2	AC	5	$4.2266T^3 + 776.81T^2 - 47325T + 956663$	$0.15 + 0.35/(1 + \exp(3.1849 - 0.04233\,T(°F)))$ a	1.747	900a	2310	2.10^{-5}c
	BC	12	$1.2248T^3 + 223.28T^2 - 13521T + 272697$	$0.15 + 0.35/$	1.566	900a	2330	2.10^{-5}c

				$(1 + \exp(3.1849 - 0.04233\ T(°F))$ a				
	LITHO	20	4300×10^6	0.4_b	0.77	900b	2140	
	LGC	20	450×10^6	0.4_b	0.67	600b	2120	

a-[27] ; b-[18] ; c-[28,30]

3. RESULTS AND DISCUSSIONS

Comment [BI13]: Results presented in Tables and Figures need to be discussed accordingly.

The model presented was simulated under extreme weather conditions. For this purpose, the hottest historical day of the year 2018, which corresponds to april 06, 2018 was chosen.

The rainy episode occurs at the time when the road surface is hottest, i.e. between 12pm and 2.30 Koudougou et al [25].

3 .1 Thermal response of the pavement during a rain event

The general pattern of simulated temperature profiles for different rainfall intensities indicates that temperatures decrease with increasing rainfall intensity (Fig. 4). This means that the induced latent and sensible heats would increase with rain intensity. This increase is induced by a cooling of the pavement, of a magnitude proportional to the intensity of the rainfall.

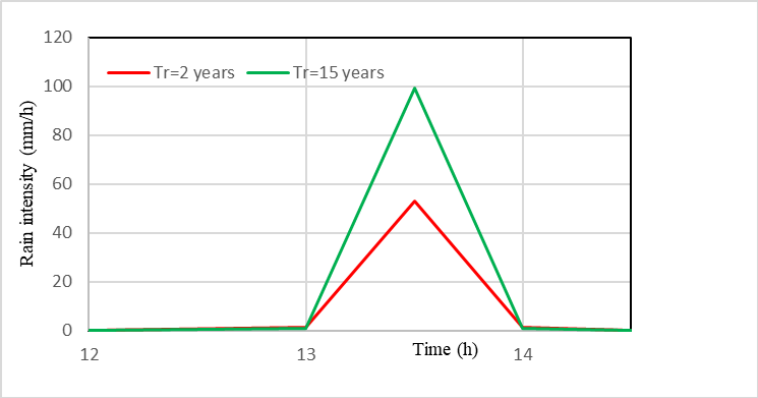

Fig. 4. Rainfall intensity profile.

The temperature profile (Fig. 5) at the surface of the roadway during rain is non-linear with respect to time, unlike the linear profile that would be obtained in the absence of rain [25].

Before the rain, the temperature profiles on the surface of the roadway, for rains with maximum intensities of 53.06 mm/h and 99 mm/h show for the two roads a difference of 0.86°C with a higher temperature for the NR4.

During rain, the surface layer of NR4 formulated with 35/50 pure bitumen cools less quickly with a difference of 0.02°C than the surface layer of NR2 formulated with 10/65 modified bitumen for an intensity maximum rainfall of 53.6 mm/h.

For a maximum rain intensity of 99 mm/h, the opposite effect with a difference of 0.03°C is observed on the road surface. This reveals the more viscous rheological character of the NR2 surface layer due to the 10/65 modified bitumen.

The proposed hygrothermal model therefore reveals that for rains with a maximum intensity of 53.6 mm/h, the rate of cooling is proportional to the rate of heating. For rains with a maximum intensity of 99 mm/h, it can be seen that the rate of cooling of the surface layer formulated with pure bitumen is greater than that formulated with modified bitumen.

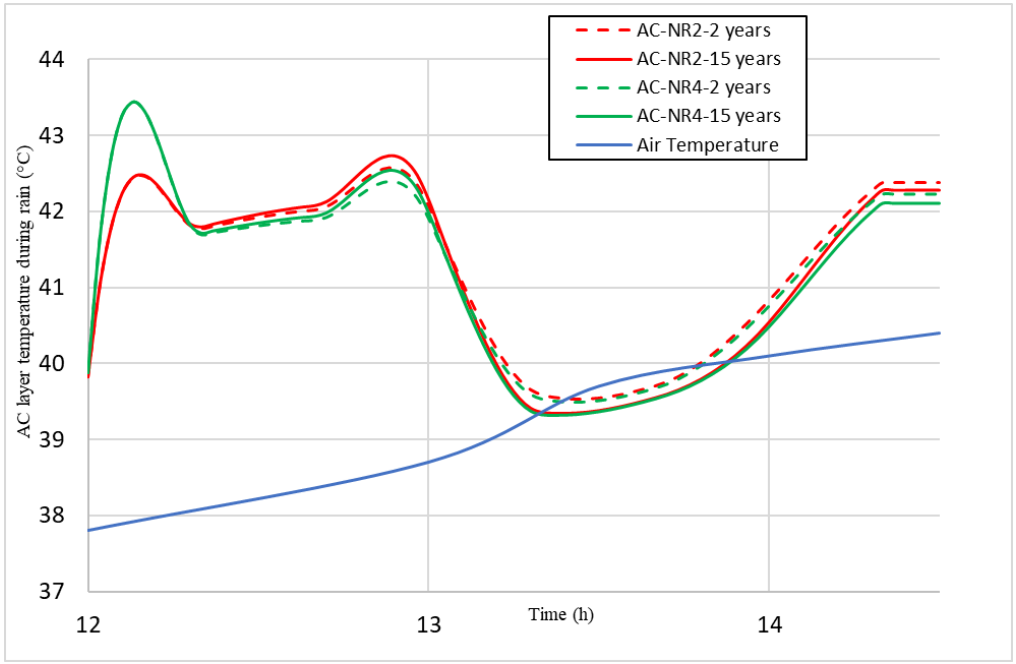

Fig. 5. Temperature profile at the pavement surface for 53.6 mm/h and 99 mm/h rainfall.

In addition, the simulated maximum temperatures soit respectivement 42.7°C et 43.4°C pour la NR2 et la NR4 (Fig. 5) are lower than the softening point temperatures of the different asphalts (Table 1).

The previous graphs show that for the duration of 2 hours and 30 min of rainfall, the order of the temperature profile in the different layers of the pavement is respected due to the long duration of the rainfall (Figs 6.a, 6.b, 6.c, 6.d).

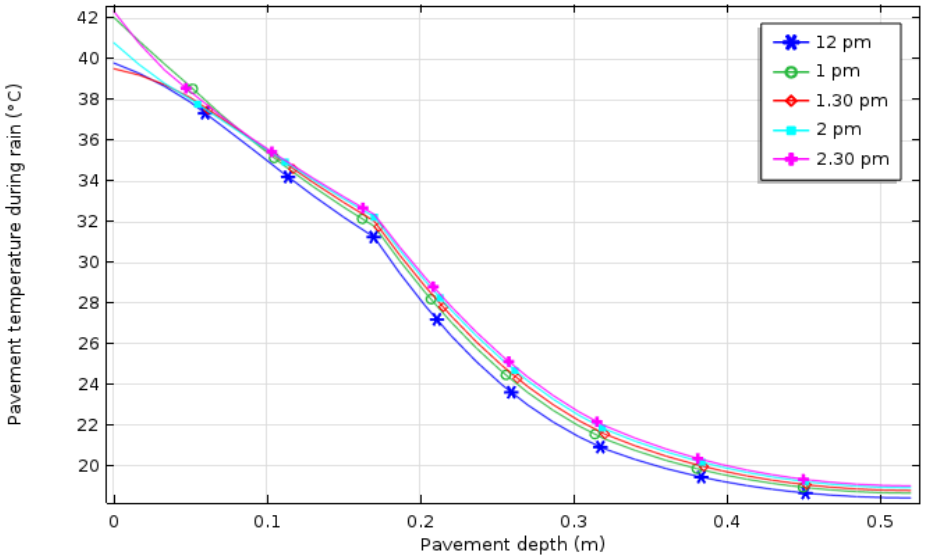

Fig. 6.a Temperature profile in the different layers of NR2 for a rainfall of maximum intensity of 53.6 mm/h.

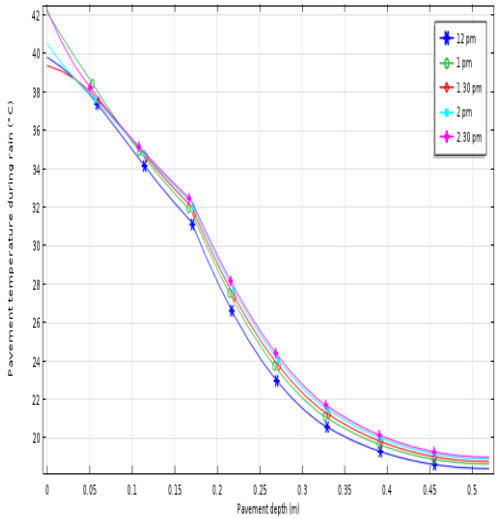

Fig. 6.b Temperature profile in the different layers of NR2 for a rainfall of maximum intensity of 99 mm/h.

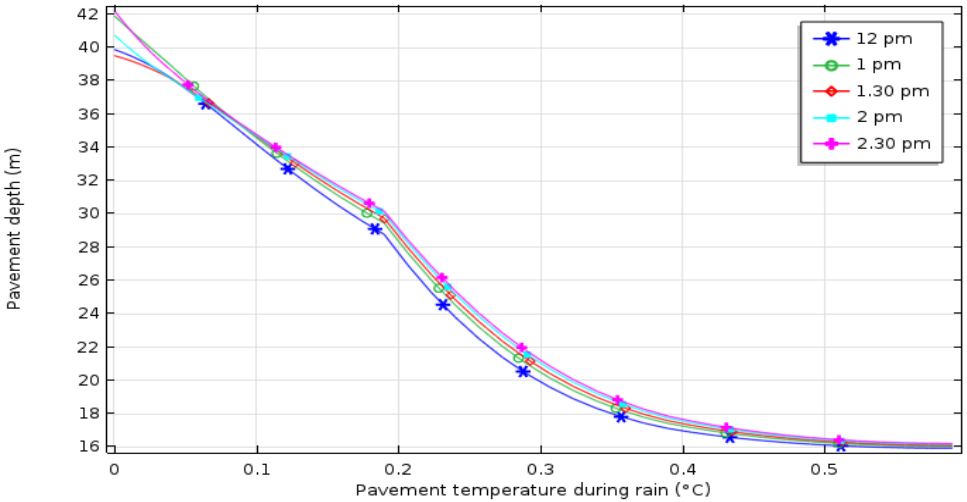

Fig. 6.c Temperature profile in the different layers of NR4 for a rainfall of maximum intensity of 53.6 mm/h.

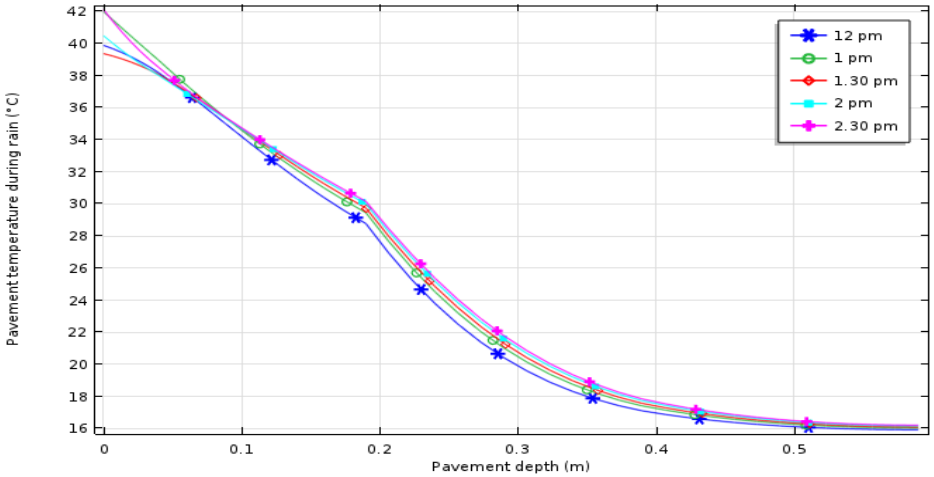

Fig. 6.d Temperature profile in the different layers of NR4 for a rainfall of maximum intensity of 99 mm/h.

The work of Kertesz et al [7] showed that during rainy periods of about 8 minutes (short duration showers), the AC surface temperature is lower than that of the BC. This could be related to the fact that latent heat exchange is greater than sensible heat exchange when rainfall is longer. While the temperature difference between AC and BC is constant during the first hour of rain, it varies in the following hours due to the greater sensitivity of AC to rain. Analysis of the above graphs of pavement surface temperatures indicates that the rain event results in lower temperatures and thus cooling of the pavement surface layer's AC and BC (Figs. 7.a, 7.b, 7.c, 7.d).

The maximum rain intensity corresponds to the simulated minimum pavement surface layer's temperatures.

Fig. 7.a Evolution of the temperature in the different layers of the NR2 during the rainfall of maximum intensity of 53.6 mm/h.

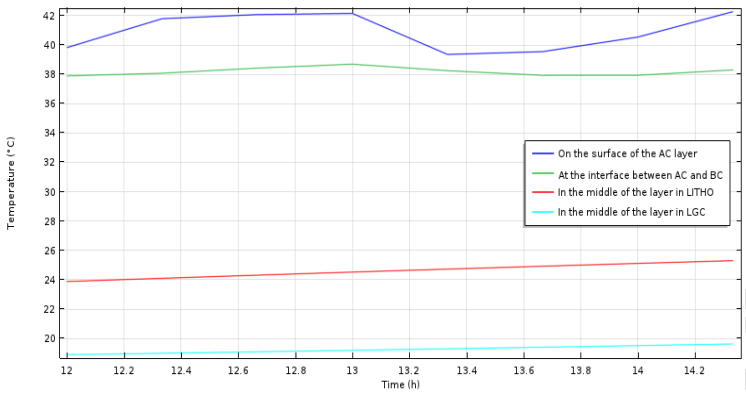

Fig. 7.b Temperature evolution in the different layers of NR2 during the maximum rainfall intensity of 99 mm/h.

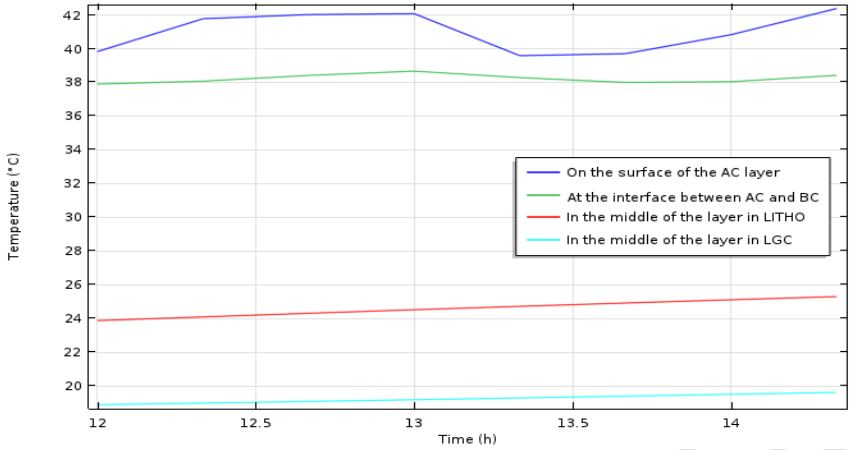

3 .2 Thermomechanical deformations of the pavement associated with a rainy event

The maximum rainfall (53.06 mm/h and 99 mm/h) intensity corresponds to the lowest temperature simulated on the pavement. The minimum deformations observed in the different layers correspond to this peak of rain intensity (t=26500s, i.e. about 13h21min30s**).** The cooling of the pavement reduces the deformations in the surface layers of the pavement **(**Figs. 8.a, 8.b, 8.c, 8.d).
The same observation is made in the lower pavement layers **(**Figs 9.a, 9.b, 9.c, 9.d**).** The deformations become more significant after the rain event. This means that the cooling phenomenon is over and the pavement continues its natural warming phenomenon related to the meteorological conditions due to solar radiation, the outside air temperature and the wind speed incident on its surface.

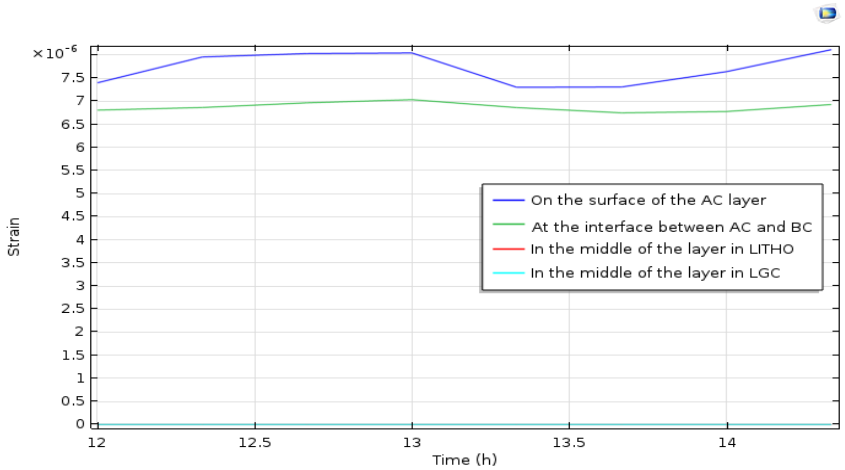

Fig. 8.a Temporal distribution of deformations according to depth in the different layers of NR2 during a rainfall of maximum intensity of 53.06 mm/h.

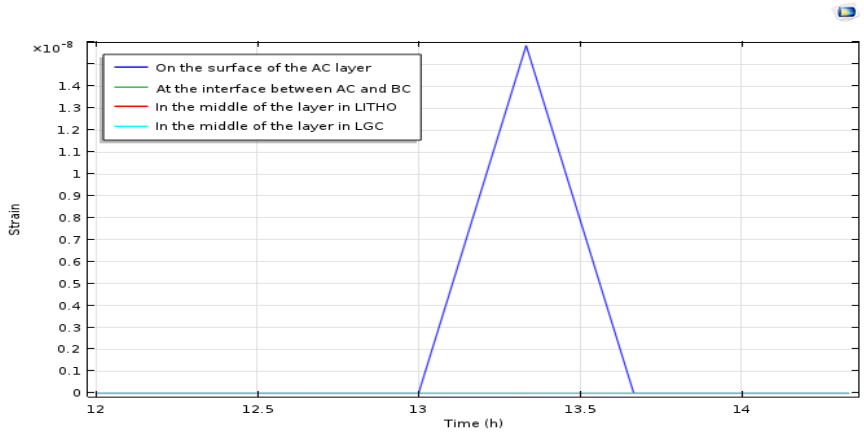

Fig. 8.b Temporal distribution of longitudinal deformations in the different layers of NR2 during a rainfall of maximum intensity of 53.06 mm/h.

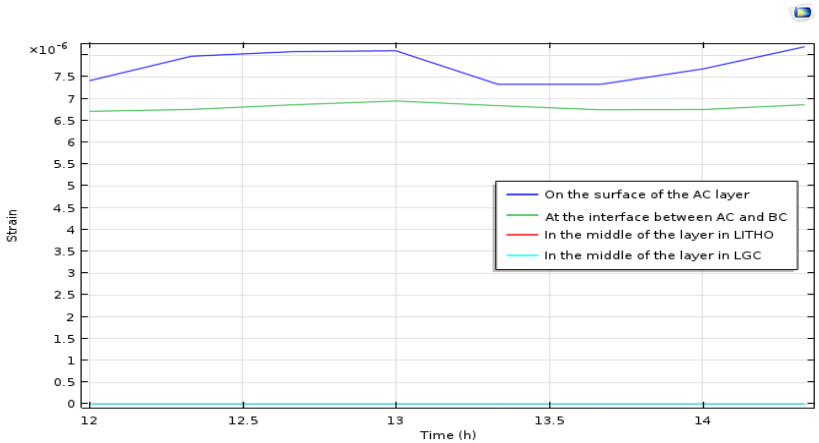

Fig. 8.c Temporal distribution of deformations according to depth in the different layers of NR2 during a rainfall of maximum intensity of 99

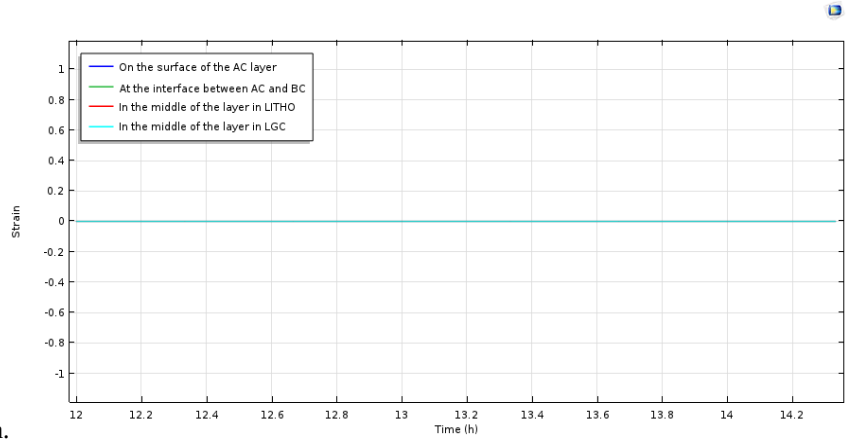

mm/h.

Fig. 8.d Temporal distribution of longitudinal deformations in the different layers of NR2 during a rainfall of maximum intensity of 99 mm/h.

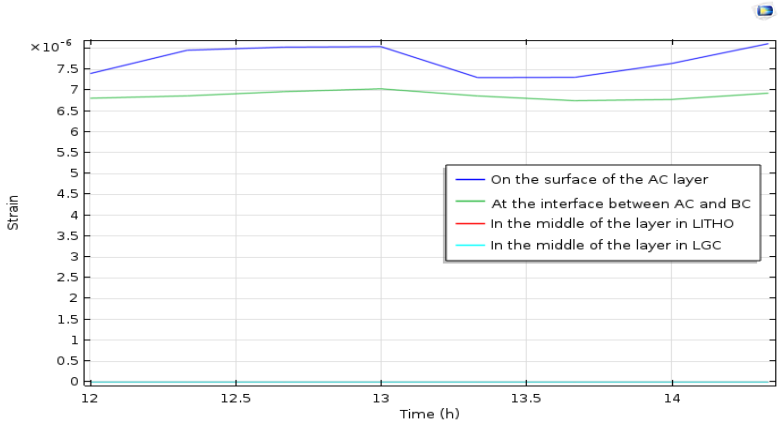

Fig. 9.a Temporal distribution of deformations according to depth in the different layers of NR2 during a rainfall of maximum intensity of 53.06

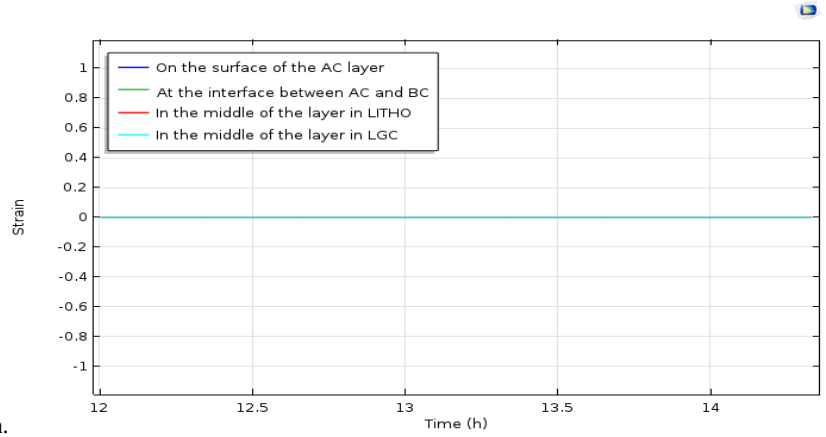

mm/h.

Fig. 9.b Temporal distribution of longitudinal deformations in the different layers of NR2 during a rainfall of maximum intensity of 53.06 mm/h.

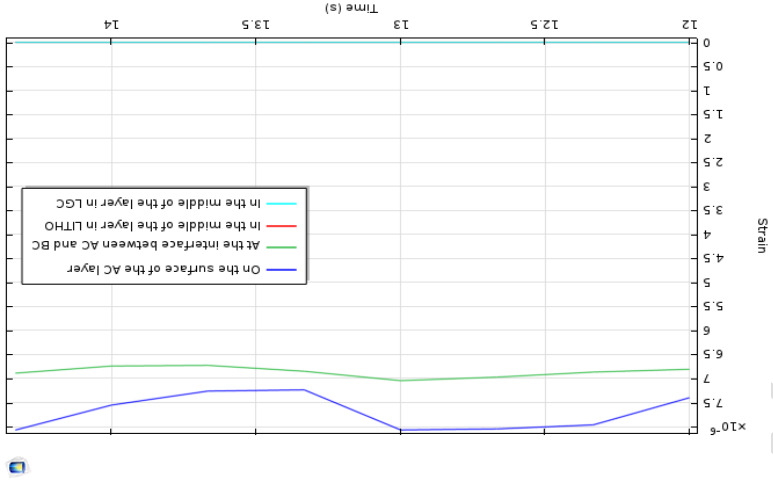

Fig. 9.c Temporal distribution of deformations according to depth in the different layers of NR4 during a shower of maximum intensity of 99 mm/h.

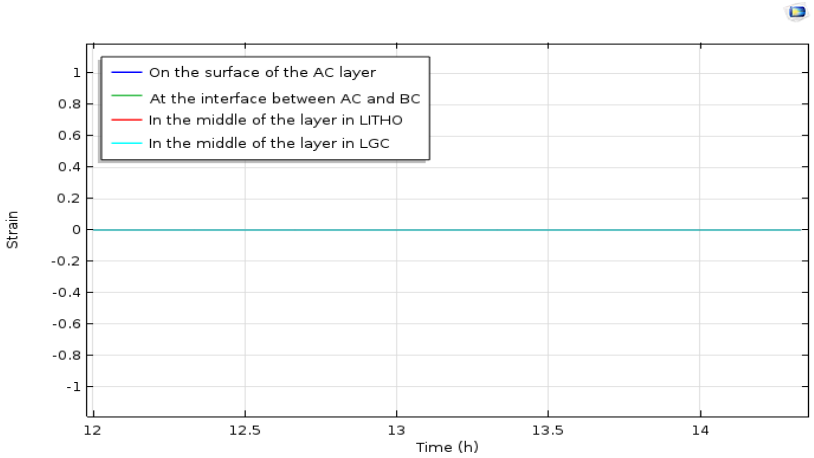

Fig. 9.d Temporal distribution of longitudinal deformations in the different layers of NR4 during a rainfall of maximum intensity of 99 mm/h.

Moreover, the maximum deformations obtained are in the range of linear elastic deformations [31] with values also lower than the permissible design values for T2 traffic pavements [32] (table 7 and table 8).

Table 7. Maximum simulated deformations in the pavement for a rainfall of 53.06 mm/h with a frequency of occurrence Tr of 2 years. ε_{xx} and ε_{zz} are respectively the longitudinal deformations and the deformations along the depth of the pavement.

Pavement	ε_{xx}	ε_{zz}	LOG (ε_{xx})	LOG (ε_{zz})
NR2	$1.6\ 10^{-8}$	$8.3\ 10^{-6}$	−7.8	−5.1
NR2	0	$7\ 10^{-6}$	-	−5.2
NR4	0	$8.2\ 10^{-6}$	-	−5.1
NR4	0	$7.1\ 10^{-6}$	-	−5.1

Table 8. Maximum simulated deformations in the pavement for a rainfall of 99 mm/h with a frequency of occurrence Tr of 15 years. ε_{xx} and ε_{zz} are respectively the longitudinal deformations and the deformations along the depth of the pavement.

Pavement	ε_{xx}	ε_{zz}	LOG (ε_{xx})	LOG (ε_{zz})
NR2	$8.2\ 10^{-6}$	$8.2\ 10^{-6}$	−5.1	−5.1
NR2	$7.2\ 10^{-6}$	$7\ 10^{-6}$	−5.1	−5.2
NR4	0	$8.2\ 10^{-6}$	-	−5.1
NR4	0	$7.1\ 10^{-6}$	-	−5.1

4. CONCLUSION

The article made it possible to highlight the difference in rheological behavior observable between mixes formulated with pure bitumen of grade 35/50 and modified bitumen of grade 10/65 according to the maximum intensity of the rain.

Comment [BI14]: Does not show the objective of the study

The resulting maximum deformations are acceptable for a T2 traffic pavement design. The rains of minimum and maximum intensity observable in Burkina Faso, the frequencies of which are 2 years and 15 years for the two types of bituminous mixes studied, do not generate permanent thermomechanical deformations that could lead to the degradation of the pavements studied. .

However, a study taking into account the phenomena of impermeability of the surface layers and the phenomena of water infiltration could certainly explain the degradations observed in the rainy season.

REFERENCES

1. Yavuzturk C, Ksaibati K. Assessment of temperature fluctuations in asphalt pavements due to thermal environmental conditions using a two-dimensional transient finite difference approach. Mountain Plains Consortium. Mpc report no. 02-136. 2002.
2. Chiasson A. D, Yavuzturk C., Ksaibati K. Linearized Approach for Predicting Thermal Stresses in Asphalt Pavements due to Environmental Conditions. Materials Civil Engineering. 20 118–27. 2008.
3. Van buren, M. A., Watt W. E., Marsalek, J., Anderson, B. Thermal enhancement of stormwater runoff by paved surfaces. Water Research, 34(4), 1359–1371. 2000.
4. Janke B. D., HerbW. R., Mohseni O., & Stefan H. G.Simulation of heat export by rainfall-runoff from a paved surface. Journal of Hydrology, 365(3–4), 195–212.2009.
5. Cohard J.M., Rosant J.M., Rodriguez F., Andrieu H., mestayer P. G., & Guillevic, P. Energy and water budgets of asphalt concrete pavement under simulated rain events. Urban Climate.2017.
6. YAvuzturk, C., Ksaibati K. Assessment of temperature fluctuations in asphalt pavements due to thermal environmental conditions using a two-dimensional, transient finite difference approach.Research Rep. No. MPC 02-136, Mountain Plains Consortium. 2005.
7. Kertesz R., SAnsalone J. Hydrologic Transport of Thermal Energy from Pavement. Journal of Environmental Engineering, 140(8), 4014028.2014.
8. Herb W., Velasquez R, Heinz Stefan, Mihai O. Marasteanu, Tim C. Simulation and Characterization of Asphalt Pavement Temperatures. Road Materials and Pavement Design, 10:1, 233-247.2009.

9. Kim K., Thompson A.M., Botter G. Modeling of thermal runoff response from an asphalt-paved plot in the framework of the mass response functions. Water Resources Research, 44(11), 1–13.2008.
10. Sansalone J,J., Teng, Z. Transient rainfall-runoff loadings to a partial exfiltration system: Implications for urban water quantity and quality. Journal of Environmental Engineering-Asce, 131(8), 1155–1167.2005.
11. Thompson M.R., Dempsey B.J., Hill H., Vogel H. Characterizing Temperature Effects for Pavement Analysis and Design. In: Transportation Research Record: Journal of the Transportation Research Board, No. 1121, Transportation Research Board of the National Academies, Washington, D.C.,pp. 14–22.1987.
12. Omidvar H., Song J., Yang J., Arwatz G, Wang Z-H, Hultmark M., Kaloush K. Modification of Urban Land Surface Temperature during Rainfall. Department of Civil and Environmental Engineering, Princeton University, Princeton, NJ.2018.
13. Lompo P.. Les Matériaux Utilisés En Construction Routière En Haute-Volta. Un Matériau Non Traditionnel.Le Lithostab. Irf Ive Conference Routiere Africaine 20-25 Janvier 1980 Nairobi. Kenya. 29-40.
14. Bourier R. Hydraulique appliquée. Le moniteur, ISBN 978-2-281-14204-4, p.127. 2018.
15. Desbordes M. Contribution à l'analyse et à la modélisation des mécanismes hydrologiques en milieu urbain. Thèse doctorat d'Etat, université des Sciences et Technologies du Languedoc, Montpellier.242 p. 1987.
16. Sighomnou D., Desbordes M. Recherche d'un modèle de pluie de projet adapté aux pré cipitations de la zone tropicale africaine ; Cas d'Adiopodoumé -Abidjan (Côte d'Ivoire). Hydrologie Continentale, n°2, pp 131-139.1988.
17. Asfour S. Récupération d'énergie dans les chaussées pour leur maintien hors gel. Phd Thesis. Université Blaise Pascal Clermont. 2017. 115 262.
18. Hall M.R.. Dehdezi P.K.. Dawson A.R.. Grenfell J.. And Isola R. Influence of the thermophysical properties of pavement materials on the evolution of temperature depth profiles in different climatic regions. Journal Of Materials In Civil Engineering. 24:32–47. 2012.
19. Sheeba J. B. Rohini.A. K. Structural And Thermal Analysis Of Asphalt Solar Collector Using Finite Element Method. Journal Of Energy. 2014.

20. Aubinet M. Longwave sky radiation parameterizations. Solar Energy. 53. 147- 154. 1994.
21. Solaimanian M.. Kennedy T.W..Predicting Maximum Pavement Surface Temperature Using Maximum Air Temperature And Hourly Solar Radiation. Transportation Research Record. Journal Of The Transportation Research Board. 1417:1–11.1993.
22. Morris.M.D. Factorial sampling plans for preliminary computational experiments. technometrics. 33(2). 161-174. 36. 1991.
23. 23.Ashrae. Ashrae handbook, fundamentals. American Society of Heating, Refrigerating and Air. 2001.Conditioning Engineers, Inc., Atlanta.
24. Di Benedetto H.. Neifar. M..Coefficients de dilatation et de contraction thermiques d'un Enrobé bitumineux avec et sans chargement Mécanique. Mechanical Tests For Bituminous Materials. Proceeding Of The 5th International Rilem Symposium Pp 421-428.1997.
25. Koudougou S.M. Toguyeni D.Y.K. modeling of pavement behavior in tropical hot and dry conditions : Numerical Approach And Comparison On Road Section. Journal of materials science & surface engineering.7(1) : 919-927. 2020.
26. Carslaw. M.S . Jaeger J.C . Conduction Of Heat In Solids.Oxford Science Publications. 1954.
27. Maher. A.. Bennert. T. A. Evaluation Of Poisson's Ratio For Use In The Mechanistic Empirical Pavement Design Guide (Mepdg).2008.
28. Mirza M. W...Development Of Relationships To Predict Poisson's Ratio For Paving Materials.. University Of Maryland. College Park. Md. Interteam Technical Report For Nchrp 1-37a. 1999.
29. Koudougou S., Tubreoumya G. , Toguyeni D., Zaida, T. Experimental Alternative to the Determination of the Thermal Dependence of the Complex Modulus of Asphalt Mixes in Dry Tropical Areas. Journal of Minerals and Materials Characterization and Engineering, 10, 275-286.2022.
30. Olard F.Comportement thermomécanique des enrobés bitumineux à basses températures. relations entre les propriétés du liant et de l'enrobé. Phd Thesis. Institut National Des Sciences Appliquées de Lyon. P138. 2003.
31. Di Benedetto H.,Nouvelle approche du comportement des enrobés bitumineux: résultats expérimentaux et formulation rhéologique, Mechanical Tests for Bituminous Mixes, Characterization, Design and Quality Control, Proceedings of the Fourth Rilem Symposium.1990.
32. Lcpc-setra., VIN P. Conception et dimensionnement des structures de chaussée. Guide technique, Paris.1994.